Selective inhibition of MCL1 overcomes venetoclax resistance in a murine model of myelodysplastic syndromes

Melissa A. Fischer,[1-2] Yuanbin Song,[3,4] Maria P. Arrate,[1] Rana Gbyli,[4] Matthew T. Villaume,[1-2] Brianna N. Smith,[1-2,5] Merrida A. Childress,[1-2] Thomas P. Stricker,[6-7] Stephanie Halene[4] and Michael R. Savona[1,2,6,8]

[1]Department of Medicine, Vanderbilt University School of Medicine, Nashville, TN, USA; [2]Cancer Biology Program, Vanderbilt University School of Medicine, Nashville, TN, USA; [3]Department of Hematologic Oncology, Sun Yat-sen University Cancer Center, State Key Laboratory of Oncology in South China, Collaborative Innovation Center for Cancer Medicine, Guangzhou, China; [4]Smilow Cancer Center, Yale University School of Medicine, New Haven, CT, USA; [5]Department of Pediatrics, Vanderbilt University School of Medicine, Nashville, TN, USA; [6]Vanderbilt-Ingram Cancer Center, Vanderbilt University School of Medicine, Nashville, TN, USA; [7]Department of Pathology, Microbiology, and Immunology, Vanderbilt University School of Medicine, Nashville, TN, USA and [8]Center for Immunobiology, Vanderbilt University School of Medicine, Nashville, TN, USA

Correspondence:
M.R. Savona
michael.savona@vanderbilt.edu

Received: January 10, 2022.
Accepted: August 11, 2022.
Prepublished: August 18, 2022.

https://doi.org/10.3324/haematol.2022.280631

Abstract

Treatment for myelodysplastic syndromes (MDS) remains insufficient due to clonal heterogeneity and lack of effective clinical therapies. Dysregulation of apoptosis is observed across MDS subtypes regardless of mutations and represents an attractive therapeutic opportunity. Venetoclax (VEN), a selective inhibitor of anti-apoptotic protein B-cell lymphoma-2 (BCL2), has yielded impressive responses in older patients with acute myeloid leukemia (AML) and high risk MDS. BCL2 family anti-apoptotic proteins BCL-X_L and induced myeloid cell leukemia 1 (MCL1) are implicated in leukemia survival, and upregulation of MCL1 is seen in VEN-resistant AML and MDS. We determined *in vitro* sensitivity of MDS patient samples to selective inhibitors of BCL2, BCL-X_L and MCL1. While VEN response positively correlated with MDS with excess blasts, all MDS subtypes responded to MCL1 inhibition. Treatment with combined VEN + MCL1 inhibtion was synergistic in all MDS subtypes without significant injury to normal hematopoiesis and reduced MDS engraftment in MISTRG6 mice, supporting the pursuit of clinical trials with combined BCL2 + MCL1 inhibition in MDS.

Introduction

Myelodysplastic syndromes (MDS) are heterogeneous bone marrow failure neoplasms marked by cytopenias, reduced quality of life and predilection to transform into acute myeloid leukemia (AML). Readily available treatments for MDS are lacking, and adapting newly approved therapies designed for AML to MDS is complicated, largely due to the heterogeneity of MDS. Despite this, and consistent with other myeloid malignancies, clonal hematopoietic stem and progenitor cells (HSPC) in MDS avoid programmed cell death often and share an imbalanced pattern of mitochondrial-controlled BCL2 family proteins.[1-4] The BCL2 family includes anti-apoptotic and pro-apoptotic proteins that compete for ligand to block or promote the activation of BAX/BAK oligomerization that is required to induce mitochondrial outer membrane potential and subsequent apoptosis.[5,6] As a method to evade apoptosis, cancer cells often upregulate anti-apoptotic proteins BCL2 and MCL1, leading to a survival advantage in numerous malignancies.[5-7] Thus, selective targeting of anti-apoptotic proteins is a viable treatment strategy. Venetoclax (VEN), a Food and Drug Administration-approved therapy that specifically inhibits the anti-apoptotic protein, BCL2, has yielded response rates of up to 50-70% in elderly AML when combined with DNA methyltransferase inhibitors (DNMTi) or low dose cytarabine,[8,9] and recently, has shown similar preliminary efficacy in higher risk MDS.[10,11] Upregulation of another BCL2 family anti-apoptotic protein, MCL1, is seen in AML and MDS treated with VEN, and is a noted mechanism of VEN resistance.[4,12-14] We previously revealed a selective MCL1 inhibitor with activity in AML patient samples dependent on MCL1 protein or resistant to BCL2 inhibition, including AML cells that arose from MDS.[13] Taken together, targeting MDS cells via inhibition of BCL2 and/or MCL1 has appeal. We determined the sensitivity of

MDS cells to inhibition of specific anti-apoptotic proteins, elucidated the characteristic determinants of response, and illustrated synergy with combined BCL2 and MCL1 inhibition both *in vitro* and *in vivo* in a murine xenograft model for MDS.

Methods

Patient and control samples

Experiments were conducted on primary MDS patient and normal (age range, 46-56 years [yr]; average, 50 yr) whole bone marrow (WBM) samples accessed from the Vanderbilt-Ingram Cancer Center Hematologic Malignancy Tumor Bank under a tissue collection protocol in accordance with the tenets of the Declaration of Helsinki and approved by the Vanderbilt University Medical Center Institutional Review Board. Normal $CD34^+$ (age range, 26-44 yr; average, 31 yr) BM cells were purchased (Lonza and Hemacare).

Drug combination calculation of synergy

The effects of S63845 + VEN were calculated using the Zero Interaction Potency (ZIP) model, which compares observed and expected combination effects.[15-17] The δ synergy score predicts the likely interaction between two drugs (<-10: antagonistic; -10 to 10: additive; >10: synergistic).

Colony-forming unit assays

Cells (preparation described below) were plated in Methocult™ H4034 Optimum (STEMCELL Technologies) at a density of 0.05-2x10^4 cells per mL in the presence of different concentrations of VEN, S63845, or S63845 + VEN compounds. Colonies were counted and identified after 12-14 days by manual observation or by using the STEMvision™ instrument and software analysis (STEMCELL Technologies). Counts were normalized per 1x10^4 MDS cells or per 500 normal $CD34^+$ cells for graphical representation.

Cell preparation for colony-forming assays

Cryopreserved MDS whole bone marrow (WBM) or normal WBM and $CD34^+$ cells were thawed and cultured in StemSpan™ (STEMCELL Technologies) + cytokines (10 ng/mL hIL3, 10 ng/mL hSCF, 5 ng/mL hIL6; Peprotech) overnight before plating cells in Methocult™ H4034 Optimum (STEMCELL Technologies). For MDS $CD34^+$ cell plating, $CD34^+$ cells were selected from WBM after thawing using the EasySep™ Human CD34 Positive Selction Kit II (STEMCELL Technologies), and then cultured as described above. Fresh MDS BM cells were treated with 100 nM VEN, 100 nM S63845, or 100 nM of each compound for S63845 + VEN treatments in the same culture conditions as the growth inhibition assays. After 24 hours of treatment, cells were plated in Methocult™ H4034 Optimum at a density of 1-2x10^4 cells per mL. After colony counts were completed, the duplicate plates for each treatment group were washed with phosphate-buffered saline + 0.5% bovine serum albumin and pooled to obtain live cell number counts via trypan blue exclusion from the methocult assays on a subset of samples.

Generation of myelodysplastic syndrome patient-derived xenotransplants

All animal experiments were approved by the Institutional Animal Care and Use Committee of Yale University. Mouse breeding: $MIS^{h/h}$TRG6 mice with homozygous knockin replacement of the endogenous mouse Csf1, Il3, Csf2, Tpo, Il6 and Sirpa with their human counterparts were bred to MITRG6 mice to generate human cytokine homozygous and hSIRPA heterozygous mice ($MIS^{h/m}$TRG6, labeled MISTRG6 throughout the study). Mice were maintained on continuous treatment with enrofloxacin in the drinking water (0.27 mg/mL, Baytril, Bayer Healthcare). MISTRG/MISTRG6 mice will be available via MTA and requests should be sent to mistrg@yale.edu.

Xenografting: newborn MISTRG6 mice (3 days of age) were X-ray irradiated (X-RAD 320 irradiator) with 2 × 150 cGy 4 hours apart. MDS patient BM CD34-selected cells were incubated with a murine anti-human CD3 antibody (clone Okt3, BioXCell) at 5 μg/100 μL for 10 minutes at room temperature prior to injection. Cells were injected intrahepatically in a volume of 20 μL with a 22-gauge Hamilton needle (Hamilton). Engraftment levels were assessed via BM aspiration at 12/ 16 weeks post-transplantation to assign treatment groups.

Statistical analysis

Data are shown as mean ± standard error of the mean (SEM) and analyzed using Prism 8 (GraphPad Software). Correlation analysis was determined using Spearman nonparametric correlation and statistical analysis was performed using an ANOVA (P<0.0001) followed by the student 2-tailed t-test. P values of <0.05 were considered to be statistically significant (n.s.: not significant, *P<0.05, **P<0.01, ***P<0.001, ****P<0.0001).

Results

Myelodysplastic syndrome subtypes are differentially sensitive to BCL2 inhibition and indiscriminately sensitive to MCL1 inhibition

We successfully cultured 35 MDS patient samples and determined their *in vitro* sensitivity to BCL2, BCL-XL and MCL1 inhibitors. Using CellTiter-Glo, we generated dose response curves and determined the 50% growth inhibitory concentrations (GI_{50}) for each inhibitor after 48 hours of exposure (Table 1). While few samples were sensitive to BCL-X_L inhibition (A-1155463), we observed a range of sen-

Venetoclax (μM)	0.23	2.54	5.00	3.69	5.00	1.05	0.25	3.61	1.41	0.29	5.00	5.00	3.82	0.84	0.27	0.23	5.00	0.25	1.57	0.27	0.20	0.47	0.26	0.11	0.36	0.18	0.15	0.12	0.08	0.14	5.00	1.15	5.00	0.18	0.13
S63845 (μM)	0.21	0.56	0.33	0.30	0.18	1.70	0.20	0.34	0.62	0.30	0.13	0.36	0.44	0.22	0.30	0.13	0.41	0.06	0.64	0.14	0.30	0.39	0.99	0.13	o.12	0.33	0.13	0.82	0.36	0.17	1.73	1.73	0.52	1.84	0.57
A-1155463 (μM)	5.00	5.00	5.00	4.00	1.46	1.70	3.17	1.68	0.53	5.00	5.00	5.00	5.00	0.58	2.99	5.00	5.00	5.00	5.00	5.00	5.00		5.00	5.00	5.00	5.00	0.03	5.00	5.00	5.00	0.12	5.00	5.00	5.00	5.00	5.00
MDS WHO 2016 Classification	MDS-RS-SLD				MDS-RS-MLD					MDS-MLD									MDS-EB1										MDS-EB2								
	MDS001	MDS002	MDS003	MDS004	MDS005	MDS006	MDS007	MDS008	MDS009	MDS010	MDS011	MDS012*	MDS013*	MDS014*	MDS015	MDS016	MDS017	MDS018	MDS019	MDS020	MDS021	MDS022	MDS023	MDS024*	MDS025	MDS026	MDS027	MDS028	MDS029#	MDS030*	MDS031	MDS032*	MDS033	MDS034	MDS035
ASXL1					■						■				■						■		■					■								
BCOR																																■	■		
BCORL1						■																													
CBL					■																										■				
DNMT3A	■					■																												■	
EZH2	■																						■												
FLT3						■																				■									
IDH1																												■							
IDH2																																		■	
NPM1																										■			■						
PTPN11																										■						■			
RUNX1						■					■							■									■				■				
SETBP1																															■				
SF3B1	■	■	■	■	■	■	■	■	■		■					■																			
SRSF2										■						■											■	■						■		
TET2	■			■	■		■		■	■	■									■			■												
TP53								■											■	■		■			■											
U2AF1					■																■														
WT1																										■			■						
% Blasts	0.0	0.0	0.3	1.5	0.0	0.0	2.0	4.0	4.0	0.0	0.0	1.0	1.0	1.5	1.5	2.0	3.0	4.5	5.0	5.0	5.0	5.0	5.0	6.0	6.0	6.0	7.0	8.5	5.0	10.0	10.0	10.0	13.0	13.0	15.0
Disease Origination	de novo	de novo	de novo	de novo	de novo	de novo	t-MDS	de novo	de novo	t-MDS	de novo	de novo	de novo	de novo	de novo	de novo	t-MDS	de novo	de novo	de novo	de novo	t-MDS	de novo	de novo	de novo	de novo	de novo	de novo	de novo	de novo	de novo	de novo	de novo	de novo	de novo	de novo
Treatment Prior to Sample Acquisition	n/a	n/a	n/a	n/a	n/a	n/a	n/a	DNMTI x12	n/a	DNMTI x4	DNMTI x5	DNMTI x1	DNMTI x16	DNMTI x16	n/a	n/a	DNMTI x3	n/a	n/a	n/a	DNMTI x5	IMID x2	Epo; DNMTI x17	DNMTI x18	n/a	n/a	n/a	n/a	n/a	n/a	DNMTI x4	n/a	DNMTI x2	n/a	DNMTI x11
Karyotype	46,XY	46,XX	45,X,-Y[15]; 46,XY[5]	46,XX	46,XX, del(20)(q11.2q13.1)	46,XY	Complex; monosomy 7	46, XY, del(5)(q22q35)[11]; 46, XY[9]	46,XX	45,X,-Y[4]; 46,XY[16]	47,XY,+14	46,XY,del(13)(q12q14)[8]; 46,XY[12]	46,XY,del(8)t(1;8)(q21;p23)	46,XY	47,XX,+19[11]; 46,XX[9]	46,XX	46,XY	45,X,-Y[4]; 44~45,XY,del(1)(q12), -21[cp2]; 46,XY[17]	46, XY,-7, +mar[14]; 46,XY[6]	46,XY,del(6)(p21.3p23)[13]; 46,XY[7]	Complex	46,XY	Complex; monosomy 7	46,XY	46,XY	Complex; monosomoy 7; del5q	46,XY	46,XY	46,XY	46,XX,-7[12]; 46,XX,[8]	47,XY,+8[2]; 46,XY[18]	47,XX,+10[10]; 47,XX,+19[2]; 46,XX[9]	46,XX,t(3;12)(q21;p13)	46,XX	46,XY

Table 1. Comprehensive data for 21 untreated, and 14 previously treated myelodysplastic syndromes (MDS) patient samples assessed is represented including growth inhibition at 50% (GI_{50}) for each inhibitor, MDS subtype by 2016 World Health Organization (WHO) classification, sample name/number, mutational status, bone marrow blast percentage, disease origination, treatment for MDS prior to sample acquisition, and karyotype. *Next generation sequencing (NGS) mutation analysis was conducted but no mutation was detected. #Patient MDS029 was considered MDS-EB2 despite only 5% blasts given the presence of Auer rods present in bone marrow aspirate. MDS017 did not have NGS performed. Other genes tested that were not detected in any of the samples include *ABL1*, *BRAF, CALR, CDKN2A, CSF3R, ETV6, FBXW7, GATA2, HRAS, JAK2, KIT, KRAS, MPL, MYD88, NRAS, PHF6, PTEN, ZRSR2*.

sitivities to BCL2 inhibition that positively correlated with blast count. Consistent with previous findings,[1,4] lower blast count MDS (RS-SLD/MLD and MLD) exhibited less sensitivity to BCL2 inhibition than higher blast count MDS subtypes (e.g., MDS-EB1; -EB2) (P=0.004) (*Online Supplementary Figure S1A*). All subtypes were sensitive to the selective MCL1 inhibitor, S63845, with decreased sensitivity in the MDS-EB2 subtype. Samples were assessed using a targeted next generation sequencing (NGS) panel of 37 commonly mutated genes in myeloid diseases. As expected, we observed an increased number of SF3B1 mutations in the lower blast count MDS with ring sideroblasts (MDS-RS) samples.[19] RAS-family mutants, particularly *PTPN11*-mutated AML have previously been shown to connote resistance to VEN.[20-24] In this cohort, one of two *PTPN11* mutant MDS samples, and two of two *CBL* mutant samples were completely resistant to BCL2 inhibition (MDS033, MDS005 and MDS031, respectively). Notably, the PTPN11 mutant sample that was not resistant to VEN (MDS026) had a low variant allele frequency (VAF) of 6% for this mutation whereas the other three RAS family mutants that demonstrated VEN-resistance all had VAF above 30%, which likely explains the lack of resistance to VEN in MDS026 (*Online Supplementary Table S1*). Otherwise, we did not observe any correlation between specific mutations and drug response in this cohort of 35 patient samples.

Dual inhibition of MCL1 and BCL2 is synergistic in all myelodysplastic syndrome samples resulting in increased apoptosis and loss of clonogenicity

In order to determine if co-inhibition of BCL2 and MCL1 is synergistic in MDS, we assessed the efficacy of three-fold dilutions of S63845 + VEN on cell viability and employed the ZIP synergy model to determine the synergistic potential.[15] The combined treatment for all samples tested resulted in an average δ synergy score >10, suggesting drug synergy (Figure 1A; *Online Supplementary Table S2*). In order to investigate if the reduced viability seen with dual inhibition of BCL2 and MCL1 led to apoptosis of MDS CD34$^+$ progenitor cells, cells were stained with anti-human CD34, Annexin V, and propidium iodide (PI) 24 hours after treatment with sub-therapeutic doses of each inhibitor (*Online Supplementary Figure S1B*). Cells treated with S63845 + VEN displayed significant reductions in MDS progenitor cells compared to VEN-treated or S63845-treated cells when all MDS samples were analyzed together (Figure 1B). Similarly, a refined analysis of MDS subtypes revealed that combined treatment significantly reduced MDS progenitors for all subtypes compared to cells treated with S63845 alone. Compared to VEN alone, the dual treatment significantly reduced MDS progenitors in RS-SLD/MLD and MLD and trended toward statistical significance for EB1 and EB2 patient samples (Figure 1C). In order to determine the long-term effects of reduced viability and increased apoptosis on clonogenicity, colony-forming unit (CFU) assays were performed. In eight tested MDS patient WBM samples, dual treatment of 100 nM S63845 + 100 nM VEN reduced CFU-granulocyte magrophage (CFU-GM) formation by 50-100%, indicating loss of clonogenicity, even in *CBL* (MDS031) or *PTPN11* (MDS033) mutant samples that were resistant to VEN monotherapy (82% and 50% reduction, respectively) (Figure 2A; *Online Supplementary Figure 2B*). This was further confirmed by trypan blue staining on cells collected from the plates of a subset of samples tested, which showed a reduction of total live cells (*Online Supplementary Figure S4*). In order to confirm dual inhibition of MCL1 and BCL2 reduced MDS HSPC, we verified this effect in CD34$^+$ cells from four MDS patient samples. Similar to the effects on WBM, dual treatment with 100 nM S63845 + 100 nM VEN reduced CFU-GM formation in MDS HSPC by 42-100%, including a *CBL* (MDS005) and *PTPN11* mutant sample that were resistant to VEN monotherapy (86% and 42%, respectively) (Figure 2A; *Online Supplementary Figure S2D*). Given the skewing toward CFU-GM colonies from the MDS samples that had been cryopreserved (*Online Supplementary Figure S2B* and *D*), we also verified the effects of S63845 + VEN treatment in freshly-obtained MDS patient samples, which corroborated a reduction, specifically, in CFU-GM colonies by 30-93% (*Online Supplementary Figure S2E*).

While 100 nM S63845 + 100 nM VEN was significantly more effective at reducing MDS WBM and HSPC colony formation, it was also toxic to normal hematopoiesis resulting in a 4-68% reduction in normal WBM CFU-GM colonies (n=8, mean 82% reduction in MDS-WBM-CFU-GM *vs*. n=4, mean 38% reduction in normal-WBM-CFU-GM, P=0.01) and a 38-69% reduction in normal CD34$^+$ CFU-GM colonies (n=4, mean 80% reduction in MDS-CD34$^+$-CFU-GM *vs*. n=7, mean 52% reduction in normal-CD34$^+$-CFU-GM, P=0.03) (Figure 2A; *Online Supplementary Figure S2A* and *C*). In order to determine a therapeutic window that would not affect normal hematopoiesis, we tested a range of doses of BCL2 + MCL1 inhibition on normal CD34$^+$ cells and found multiple dose combinations that had no significant impact on colony formation (Figure 2B). We reduced the original tested concentration by 50% and assessed dual treatment of 50 nM S63845 + 50 nM VEN, which exemplified the selective targeting of MDS compared to normal WBM cells (n=6, mean 50% reduction in MDS-WBM-CFU-GM *vs*. n=4, mean 0% reduction in normal-WBM-CFU-GM, P=0.0002) and HSPC (n=4, mean 71% reduction in MDS-CD34$^+$-CFU-GM *vs*. n=2, mean 0% reduction in normal-CD34$^+$-CFU-GM, P=0.02) (Figure 2C; *Online Supplementary Figure S3A to D*). Markedly, all MDS WBM and CD34$^+$ samples displayed reduced CFU-GM colony formation using either high (100 nM S63835 + 100 nM VEN) or low (50 nM S63845 + 50 nM VEN)

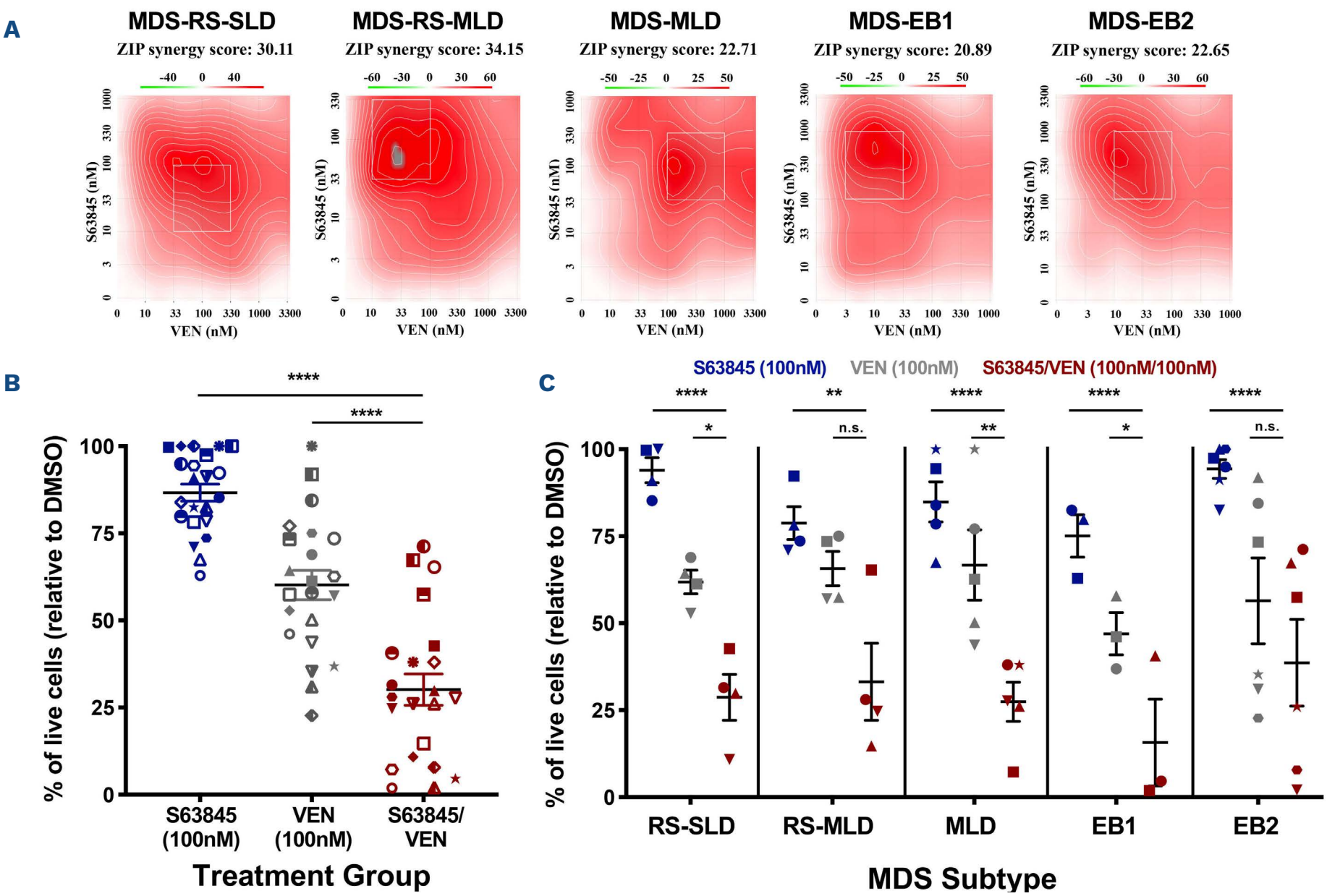

Figure 1. Dual inhibition of MCL1 and BCL2 is synergistic in myelodysplastic syndrome cells resulting in increased apoptosis. (A) Cell viability of primary myelodysplastic syndrome (MDS) samples was measured by CellTiter-Glo at 48 hours after treatment with three-fold dilutions of S63845, venetoclax (VEN) or a combination of both. Contour plots of synergy scores generated from the cell viability dose matrix of S63845 and VEN using the zero interaction potency (ZIP) model. The synergy scores were represented by pseudocoloring 2-D contour plots over the dose matrix, giving rise to the overall synergy landscape. Red color indicates synergy, while green color indicates antagonism for the various concentrations of the S63845/VEN combination (note different pseudocoloring scale for ZIP synergy scores between the samples). (B and C) Apoptosis in $CD34^+$ cells was measured by annexin V/PI staining using flow cytometry after 24 hours of treatment in all samples combined (B) or broken down into MDS subtypes; MDS-RS-SLD is MDS with ring sideroblast with single lineage dysplasia; MLD is multi-lineage dysplasia; EB1 is excess blasts 5-9%; EB2 is 10-19% blasts (C). The percent of live cells relative to DMSO control were calculated. Statistical comparisons between S63845 or VEN monotherapy and the combination are shown (ANOVA followed by two-tailed *t*-test; n.s.: not significant, **P*<0.05, ***P*<0.01, ****P*<0.001, *****P*<0.0001).

combination therapy, even VEN-monotherapy-resistant (GI50 >5 μM) samples (*Online Supplementary Table S3*).

Combined MCL1 and BCL2 inhibition reduces human myelodysplastic syndrome cell engraftment in MISTRG6 mice

We further validated the efficacy of S63845 + VEN combination treatment using *in vivo* MDS patient-derived xenotransplants (PDX). We have previously shown successful establishment of MDS PDX with faithful clonal representation in cytokine humanized 'MISTRG' mice. MISTRG mice carry humanized alleles for M-$CSF^{h/h}$, IL-3/GM-$CSF^{h/h}$, SIR-$P\alpha^{h/m}$, and $TPO^{h/h}$, on the $RAG2^{-/-}$ $\gamma c^{-/-}$ background, and are viable, healthy and fertile. Gene-humanizations via knockin significantly improve the engraftment, differentiation and maintenance of human cells from MDS and other hematologic malignancies.[25-27] As MDS is an inflammatory disorder with elevated IL-6 levels and is highly dependent on its microenvironment,[28,29] we made use of a next-generation version of MISTRG with humanization via targeted insertion of human interleukin-6 (*IL-6*), in short, 'MISTRG6'. MISTRG6 have been shown recently to efficiently engraft healthy human $huCD34^+$ and myeloma cells.[26,30] Before testing the effects of combined BCL2 and MCL1 inhibition experiments in MDS PDX, we performed toxicity evaluations in MISTRG6 mice. Mice were treated with vehicle, VEN (15 mg/kg; 5 days on, 2 days off), or a combination of VEN (15 mg/kg; 5 days on, 2 days off) and S63845 (12.5 mg/kg; 2 days on, 5 days off) for a total of 2 weeks. Measurements were taken prior to starting treatment (Pre), 1 week, and 2 weeks after treat-

ment to determine weight, red blood cell count, hemoglobin, white blood cell count, and platelet count. No detrimental effects were seen on the mouse hematopoietic cells in MISTRG6 mice (*Online Supplementary Figure S5*). Next, we confirmed engraftment of selected MDS patient samples from Table 1 that had sufficient cells to perform *in vivo* studies. All three samples engrafted in the MISTRG6 mice, at varying levels in the bone marrow (BM) (Figure 3A and B), and were largely comprised of the myeloid lineage (Figure 3C). In order to maximize the information we could obtain with this limited resource, we used these test engraftment mice to perform a pilot study comparing vehicle treatment to combined BCL2 + MCL1 inhibition. This preliminary experiment suggested that dual treatment would decrease MDS engraftment in the BM (*Online Supplementary Figure S6*).

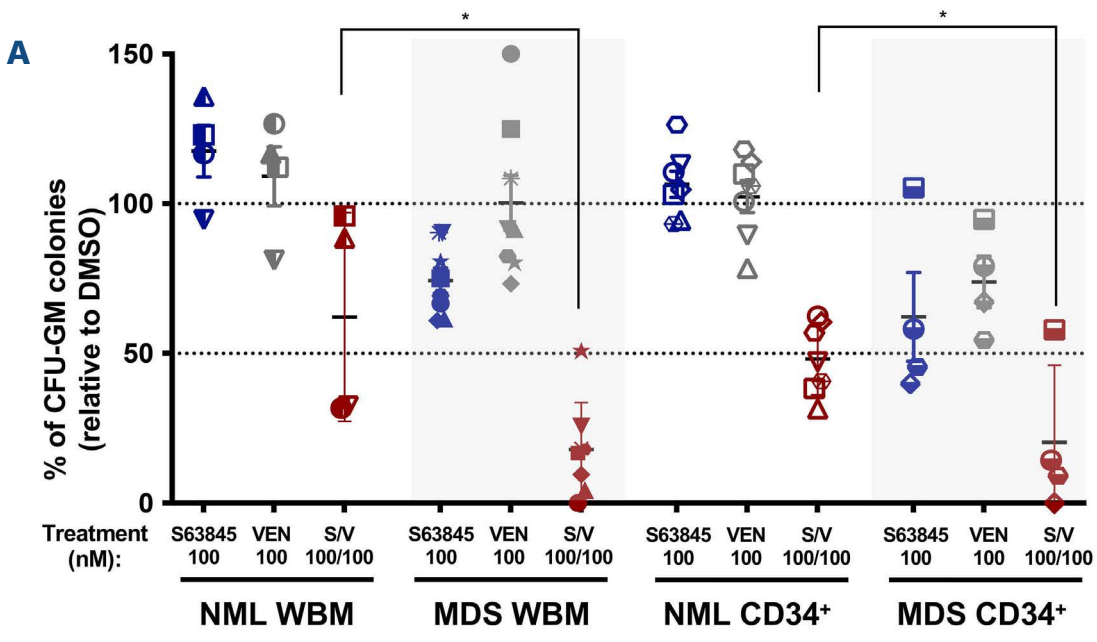

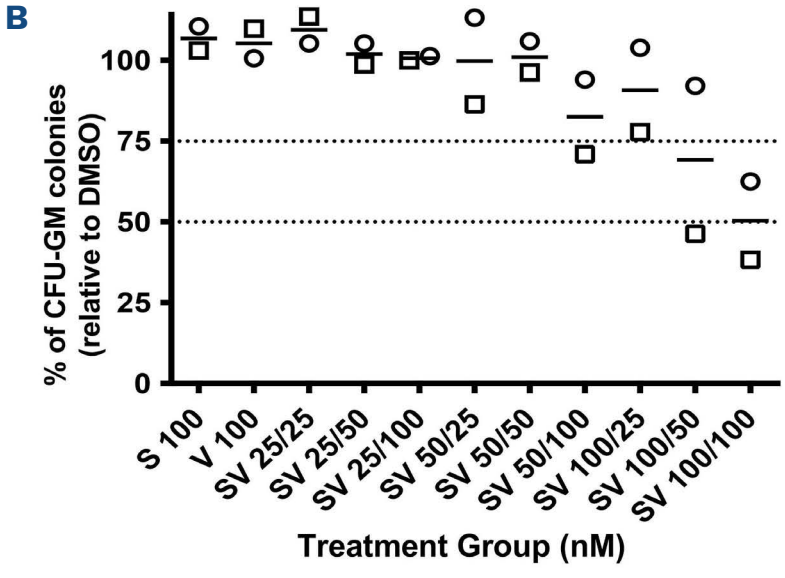

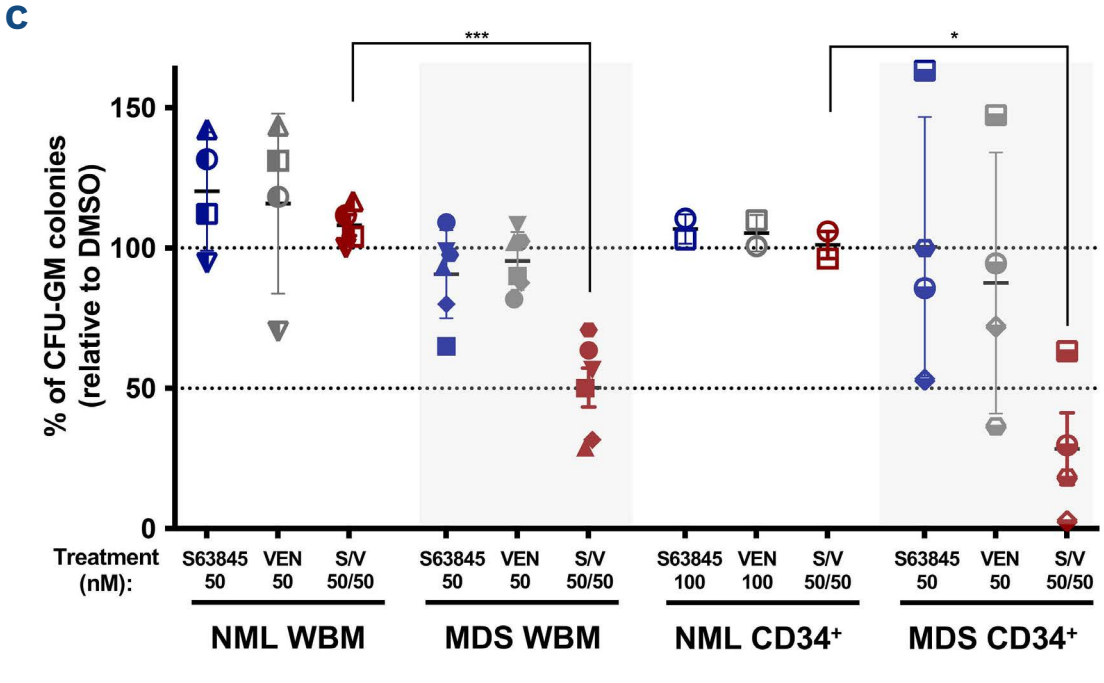

Figure 2. Combined inhibition of MCL1 and BCL2 reduces clonogenicity at doses that are tolerable to normal hematopoietic stem and progenitor cells. (A) Colony forming assays of normal (NML) whole bone marrow (WBM), MDS WBM, NML CD34$^+$, and MDS CD34$^+$ patient cells. The percent of CFU-GM colonies relative to dimethyl sulfoxide (DMSO) for 100 nM S63845, 100 nM venetoclax (VEN), or S/V (100 nM S63845 + 100 nM VEN) treatment groups were calculated. Statistical comparisons of S/V combination treatment between NML WBM *vs.* MDS WBM and NML CD34$^+$ *vs.* MDS CD34$^+$ cells are shown (two-tailed *t*-test; **P*<0.05). (B) Colony-forming assays of NML CD34$^+$ cells treated with a range of combined concentrations of S63845 + VEN (SV). The percent of CFU-GM colonies relative to DMSO were calculated. (C) Colony-forming assays of normal (NML) whole bone marrow (WBM), MDS WBM, NML CD34$^+$, and MDS CD34$^+$ patient cells. The percent of CFU-GM colonies relative to DMSO for 50 nM S63845, 50 nM VEN, or S/V (50 nM S63845 + 50 nM VEN) treatment groups were calculated. Statistical comparisons of S/V combination treatment between NML WBM *vs.* MDS WBM and NML CD34$^+$ *vs.* MDS CD34$^+$ cells are shown (two-tailed *t*-test; **P*<0.05; ****P*<0.001). CFU-GM is colony-forming unit – granulocyte, macrophage. Data in (A) and (C) is represented as mean ± standard error of the mean, and individual patient samples in (A to C) are represented by unique symbols.

In vitro assays showed patient sample MDS019 was resistant to VEN treatment alone (Table 1; GI_{50} =1.6 μM), but responded to dual BCL2+MCL1 inhibition (*Online Supplementary Table S2*; average ZIP δ synergy score =21.6). Since MDS019 also led to the most consistent engraftment (Figure 3A and B), we tested this sample to determine if combined BCL2 + MCL1 inhibition could also overcome VEN resistance *in vivo*. Remaining cells from MDS019 (MDS-EB1 subtype) were allowed to engraft in MISTRG6 mice for 16 weeks before beginning treatment with vehicle, VEN (15 mg/kg; 5 days on, 2 days off), or a combination of VEN (15 mg/kg; 5 days on, 2 days off) and S63845 (12.5 mg/kg; 2 days on, 5 days off) for a total of 4 weeks (n=4 per treatment group). The percent or total number of human CD45$^+$ (huCD45$^+$) cells in the BM were compared between pre- and post-treatment for each treatment group (Figure 4A and B, respectively). VEN single treatment reduced the number of huCD45 cells in the BM but displayed a marked increase in the percent of huCD45 cells similar to mice treated with vehicle. Conversely, both of these analyses demonstrated a striking reduction in percent and number of huCD45$^+$ cells in the BM after combined BCL2+MCL1 inhibition, with almost a complete loss of huCD45$^+$ cells. Furthermore, after the completion of the treatment, measurement of the percent of huCD45$^+$/lin$^-$/huCD38$^-$/huCD34$^+$ HSPC in the BM (Figure 4C) indicated this combined treatment, but not VEN treatment alone, was successful at specifically reducing the MDS-HSPC that are known to drive the propagation of MDS. This finding was further exemplified by reduced CD34$^+$ staining by immunohistochemistry in the bone marrow of mice treated with dual BCL2 + MCL1 inhibition (Figure 4D). Notably, these results are consistent with the outcome of the *in vitro* proliferation assays for MDS019 patient cells.

Discussion

The study of MDS HSPC *in vitro* is challenging. MDS cell lines are limited, contrived and not representative of MDS, particularly lower risk MDS, so patient samples are required.[31-33] *Ex vivo* study of MDS patient samples is also limited by sample heterogeneity, availability, and the practical consideration of how few cells are available in the setting of a disease characterized by marrow failure. Nonetheless, we have performed a comprehensive analysis on a cohort of MDS patient samples to investigate the value of targeting anti-apoptotic proteins for the treatment of MDS. Our data validated previous findings that higher blast count MDS subtypes (EB1 and EB2) are more sensitive to VEN monotherapy than low blast count subtypes.[1,4] We illustrated that mutations associated with VEN resistance in AML may be similarly relevant in MDS, and also discovered, importantly, that MCL1

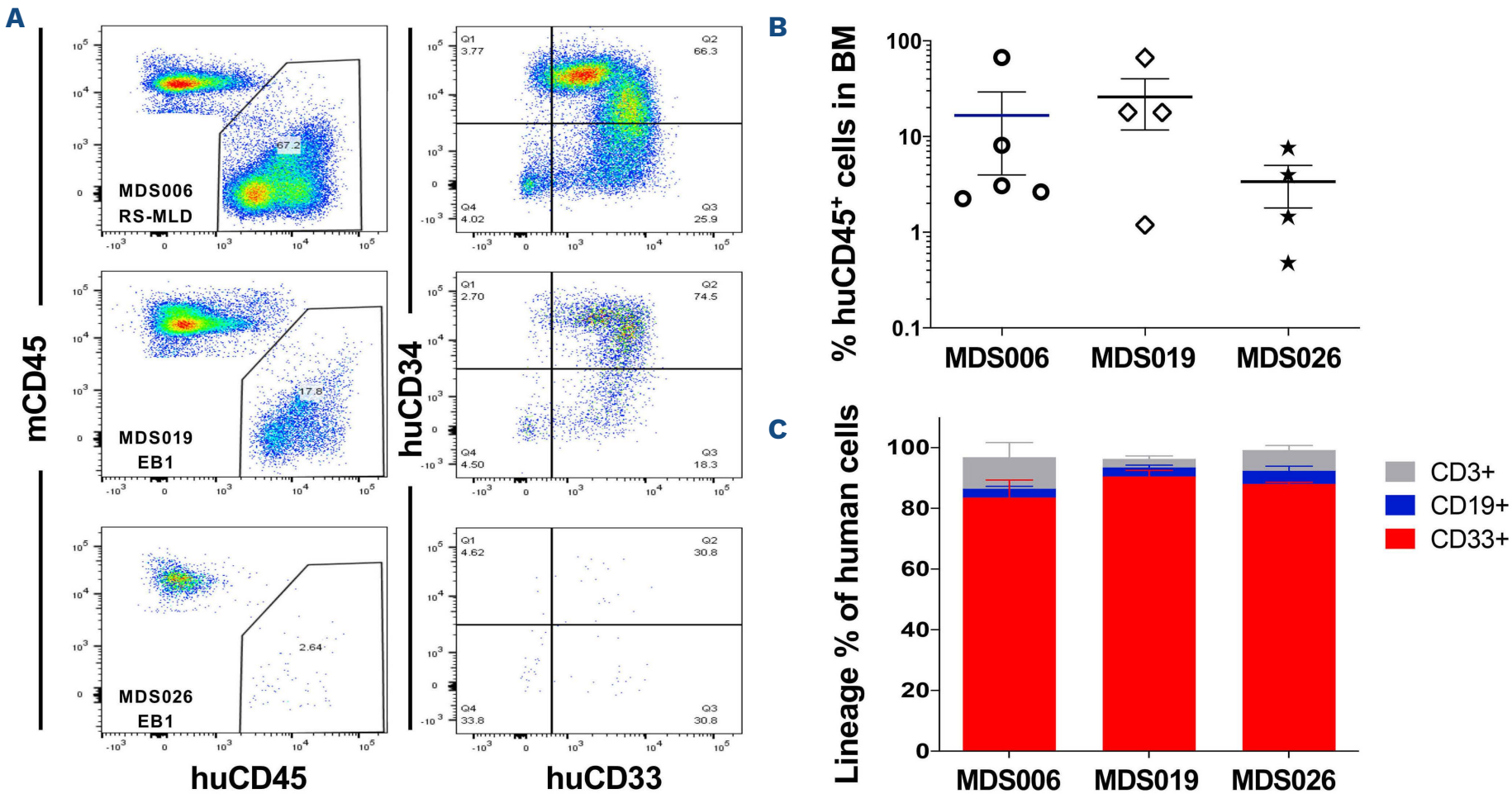

Figure 3. Myeloid engraftment of low and medium-risk myelodysplastic syndromes in MISTRG6 mice. (A to C) Confirmed engraftment of 3 primary myelodysplastic syndrome (MDS) patient cells in MISTRG6 mice. (A) Flow cytometric analysis of mouse *vs.* human CD45 (mCD45 *vs*. huCD45; left panels) and huCD34 *vs*. huCD33 (right panels). (B) Percent of huCD45$^+$ cells in the bone marrow (BM) for each patient sample. (C) Relative distribution of myeloid CD33$^+$ (red), B-lymphoid CD19$^+$ (blue), and T-lymphoid CD3$^+$ (gray) cells as percent of human CD45$^+$ cells for each patient sample.

inhibtion may be effective for all MDS subtypes. Moreover, drug synergy from combining BCL2 and MCL1 inhibitors can be achieved across all subtypes and mutational profiles of MDS in this model, even in the presence of RAS family mutations that are believed to confer resistance to VEN monotherapy (e.g., *CBL* and *PTPN11* in this cohort).[20-24]

The *in vivo* reduction of MDS progenitor cells in the BM from MDS PDX is the first successful test of selective anti-apoptotic inhibitors in an *in vivo* MDS PDX model. Prior patient-derived MDS xenograft models have demonstrated inefficient engraftment potential in multiple murine backgrounds and often do not recapitulate the disease characteristics.[32,34-42] Other studies have shown mixed results when attempting to improve MDS cell engraftment into mice with co-injection of normal or MDS patient-derived mesenchymal stromal cells.[40,42] The MISTRG mice overcame the obstacles presented by other models by expressing human cytokines in place of their murine counterparts at the endogenous locus to provide physiological expression of these human cytokines and MISTRG6 mice further provide the otherwise non-crossreactive critical inflammatory cytokine, IL-6, which is over-expressed in mesenchymal stromal cells in MDS and other hematologic malignancies.[25] Building on this model allowed us to demonstrate successful engraftment of MDS patient cells in MISTRG6 mice for the first time, and to test the effects of anti-apoptotic inhibitors *in vivo*.

Xenografting of human MDS is improved with the MISTRG6 model, yet a finite number of patient samples with robust cellular engraftment hindered the number of transplants. Nonetheless, these MDS PDX experiments edify findings

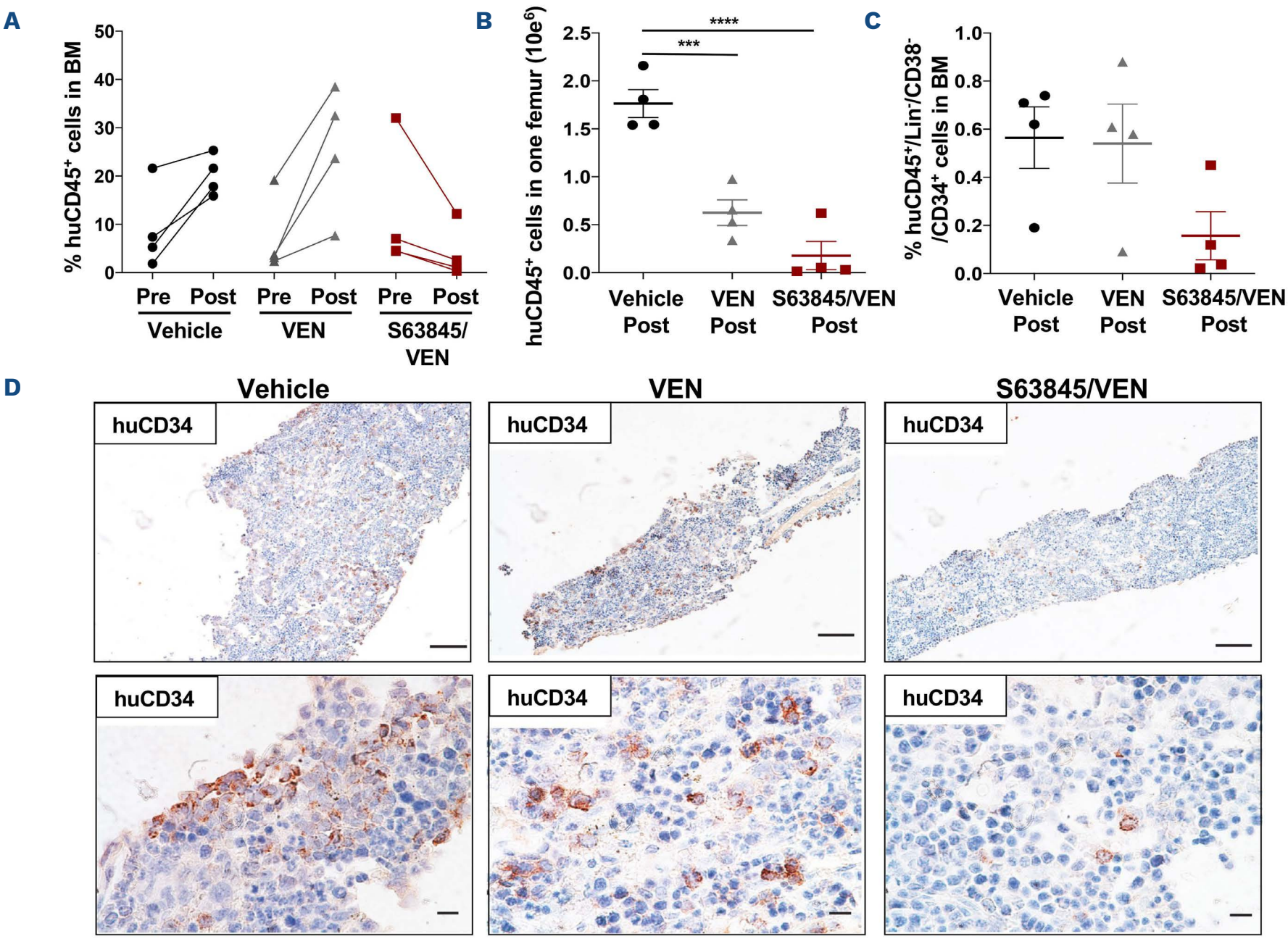

Figure 4. Evidence of reduced myelodysplastic syndrome engraftment in MISTRG6 mice after co-inhibition of BCL2 and MCL1. (A to D) Patient sample MDS019-EB1 was allowed to engraft in MISTRG6 mice for 16 weeks before beginning treating with vehicle, venetoclax (VEN) (15 mg/kg; 5 days on, 2 days off), or a combination of VEN (15 mg/kg; 5 days on, 2 days off) and S63845 (12.5 mg/kg; 2 days on, 5 days off) for a total of 4 weeks (n=4 per treatment group). The percent (A) or total number (B) of huCD45$^+$ cells in the bone marrow (BM) were compared between pre and post-treatment for each treatment group. (C) After completion of the treatment, the percent of huCD45$^+$/lin$^-$/huCD38$^-$/huCD34$^+$ in the BM was determined. (D) Representative histologic images of BM from mice in (A to C) that were treated with vehicle, VEN, or S63845/VEN and underwent immunohistochemical staining for huCD34 (top panel, original magnification 10x, scale bars: 100 μm; lower panel, original magnification 60x, scale bars:10 μm). The data in (B and C) are represented by mean ± standard error of the mean, and statistical comparisons between vehicle and VEN or combination treatments are shown (two-tailed *t*-test; n.s.: not significant, **P*<0.05, ***P*<0.01, ****P*<0.001).

from our *ex vivo* studies to illustrate the selective utility of BCL2 inhibitor monotherapy in MDS and provide promise for the use of combined BCL2 + MCL1 inhibition for the treatment of all MDS subtypes, particularly in patients who may be resistant to VEN monotherapy.

BCL2 inhibition has changed the standard of care in myeloid malignancies; refining the design of clinical trials testing BCL2 and MCL1 inhibitors in MDS and the precision of patient selection for therapy is a top therapeutic priority. While combination of BCL2 and MCL1 inhibition may have a dose-dependent impact on normal hematopoiesis, experimental evidence seems to indicate that toxicity on normal $CD34^+$ cells is limited at clinically meaningful doses *in vivo*[13] and *in vitro*,[43] as we have also shown here. The data presented here suggest dual BCL2 + MCL1 inhibition should be considered for the treatment of all MDS subtypes regardless of mutational status, even those with mutations that may be less likely to respond to VEN monotherapy (e.g., *TP53* or *RAS* family mutations),[20-24] and carefully designed clinical trials with flexible dosing schedules amenable to MDS are warranted.

Disclosures

MRS has served on consultancy/advisory board/data safety monitoring committees for Abbvie, BMS, CTI, Forma, Geron, Karyopharm, Novartis, Ryvu, Sierra Oncology, Takeda, Taiho TG Therapeutics; has equity in Karyopharm; and his institution has received research funding from ALX Oncology, Incyte, Takeda, and TG Therapeutics. SH serves on the advisory board of FORMA Therapeutics.

Contributions

MAF, YS, and RG designed and performed experiments. MPA, and MTV performed experiments. MAF, YS, RG, MPA, MTV, MAC, BNS, TPS, SH, and MRS analyzed data. MAF and MRS performed statistical analysis and wrote the manuscript. SH and MRS designed and supervised the study. All authors reviewed and edited drafts of the manuscript and approved the final version of the manuscript.

Acknowledgments

For the in vivo studies, we thank Yale Pathology Tissue Services, especially A. Brooks for research histology services, Yale Animal Resources Center, especially P. Ranney, J. Fonck for animal care, and Yale Flow Cytometry Core, especially Lesley Divine, Diane Trotta and Chao Wang for flow cytometry analysis.

Funding

This work was generously supported by the Edward P. Evans Foundation (2017-11), Beverly and George Rawlings Directorship, the Biff Ruttenberg Foundation, the Adventure Alle Fund, and the Leukemia and Lymphoma Society (2321-19) for which, MRS is a Clinical Scholar. MRS was supported by the NCI (R01CA262287-01). SH was supported by the NIH/NIDDK (R01DK102792), the Frederick A. Deluca Foundation, the Edward P. Evans Foundation, and the Department of Defense. YS was supported by a pilot grant from the Yale Cooperative Center of Excellence in Hematology (YCCEH) and the National Natural Science Foundation of China (General Program No. 82170137). BNS was supported by the NCI (5K12CA090625). This study was in part supported by the Animal Modeling Core of the Yale Cooperative Center of Excellence in Hematology (NIDDK U54DK106857). Patient samples were garnered from the Vanderbilt-Ingram Cancer Center (VICC) Hematologic Malignancy Tumor Bank. The Vanderbilt-Ingram Cancer Center grant (NCI P30 CA068485-19) supported this work. The REDCap database tool is supported by grant UL1 TR000445 from NCATS/NIH. Flow Cytometry experiments were performed in the VUMC Flow Cytometry Shared Resource. The VUMC Flow Cytometry Shared Resource is supported by the Vanderbilt Ingram Cancer Center (P30 CA68485) and the Vanderbilt Digestive Disease Research Center (DK058404).

Data-sharing statement

Not applicable as data generated in this study have been included in the published article.

References

1. Reidel V, Kauschinger J, Hauch RT, et al. Selective inhibition of BCL-2 is a promising target in patients with high-risk myelodysplastic syndromes and adverse mutational profile. Oncotarget. 2018;9(25):17270-17281.
2. Parker JE, Mufti GJ, Rasool F, Mijovic A, Devereux S, Pagliuca A. The role of apoptosis, proliferation, and the Bcl-2-related proteins in the myelodysplastic syndromes and acute myeloid leukemia secondary to MDS. Blood. 2000;96(12):3932-3938.
3. Invernizzi R, Pecci A, Bellotti L, Ascari E. Expression of p53, bcl-2 and ras oncoproteins and apoptosis levels in acute leukaemias and myelodysplastic syndromes. Leuk Lymphoma. 2001;42(3):481-489.
4. Jilg S, Reidel V, Muller-Thomas C, et al. Blockade of BCL-2 proteins efficiently induces apoptosis in progenitor cells of high-risk myelodysplastic syndromes patients. Leukemia. 2016;30(1):112-123.
5. Bhola PD, Letai A. Mitochondria - judges and executioners of cell death sentences. Mol Cell. 2016;61(5):695-704.
6. Letai A, Bassik MC, Walensky LD, Sorcinelli MD, Weiler S, Korsmeyer SJ. Distinct BH3 domains either sensitize or activate mitochondrial apoptosis, serving as prototype cancer therapeutics. Cancer Cell. 2002;2(3):183-192.
7. Hanahan D, Weinberg RA. Hallmarks of cancer: the next generation. Cell. 2011;144(5):646-674.
8. DiNardo CD, Pratz K, Pullarkat V, et al. Venetoclax combined with decitabine or azacitidine in treatment-naive, elderly patients with acute myeloid leukemia. Blood. 2019;133(1):7-17.

9. Wei AH, Strickland SA, Hou J-Z, et al. Venetoclax combined with low-dose venetoclax for previously untreated patients with acute myeloid leukemia: results from a phase Ib/II study. J Clin Oncol. 2019;37(15):1277-1284.
10. Ball BJ, Famulare CA, Stein EM, et al. Venetoclax and hypomethylating agents (HMAs) induce high response rates in MDS, including patients after HMA therapy failure. Blood Adv. 2020;4(13):2866-2870.
11. Zeidan AP, DA, Garcia, JS, et al. A phase 1b study evaluating the safety and efficacy of venetoclax in combination with azacitidine for the treatment of relapsed/refractory myelodysplastic syndrome. Blood. 2020;134(Suppl 1):S565.
12. Pan R, Ruvolo VR, Wei J, et al. Inhibition of Mcl-1 with the pan-Bcl-2 family inhibitor (-)BI97D6 overcomes ABT-737 resistance in acute myeloid leukemia. Blood. 2015;126(3):363-372.
13. Ramsey HE, Fischer MA, Lee T, et al. A novel MCL1 inhibitor combined with venetoclax rescues venetoclax-resistant acute myelogenous leukemia. Cancer Discov. 2018;8(12):1566-1581.
14. Konopleva M, Pollyea DA, Potluri J, et al. Efficacy and biological correlates of response in a phase II study of venetoclax monotherapy in patients with acute myelogenous leukemia. Cancer Discov. 2016;6(10):1106-1117.
15. Yadav B, Wennerberg K, Aittokallio T, Tang J. Searching for drug synergy in complex dose-response landscapes using an interaction potency model. Comput Struct Biotechnol J. 2015;13:504-513.
16. Ianevski A, He L, Aittokallio T, Tang J. SynergyFinder: a web application for analyzing drug combination dose-response matrix data. Bioinformatics. 2017;33(15):2413-2415.
17. Ianevski A, Giri AK, Aittokallio T. SynergyFinder 2.0: visual analytics of multi-drug combination synergies. Nucleic Acids Res. 2020;48(W1):W488-W493.
18. Consortium APG. AACR Project GENIE: Powering Precision Medicine through an International Consortium. Cancer Discov. 2017;7(8):818-831.
19. Malcovati L, Papaemmanuil E, Ambaglio I, et al. Driver somatic mutations identify distinct disease entities within myeloid neoplasms with myelodysplasia. Blood. 2014;124(9):1513-1521.
20. Pei S, Pollyea DA, Gustafson A, et al. Monocytic subclones confer resistance to venetoclax-based therapy in patients with acute myeloid leukemia. Cancer Discov. 2020;10(4):536-551.
21. Chyla B, Daver N, Doyle K, et al. Genetic biomarkers of sensitivity and resistance to venetoclax monotherapy in patients with relapsed acute myeloid leukemia. Am J Hematol. 2018;93(8):E202-E205.
22. DiNardo CD, Tiong IS, Quaglieri A, et al. Molecular patterns of response and treatment failure after frontline venetoclax combinations in older patients with AML. Blood. 2020;135(11):791-803.
23. Chen X, Glytsou C, Zhou H, et al. Targeting mitochondrial structure sensitizes acute myeloid leukemia to venetoclax treatment. Cancer Discov. 2019;9(7):890-909.
24. Nechiporuk T, Kurtz SE, Nikolova O, et al. The TP53 apoptotic network is a primary mediator of resistance to BCL2 inhibition in AML Cells. Cancer Discov. 2019;9(7):910-925.
25. Song Y, Rongvaux A, Taylor A, et al. A highly efficient and faithful MDS patient-derived xenotransplantation model for pre-clinical studies. Nat Commun. 2019;10(1):366.
26. Das R, Strowig T, Verma R, et al. Microenvironment-dependent growth of preneoplastic and malignant plasma cells in humanized mice. Nat Med. 2016;22(11):1351-1357.
27. Saito Y, Ellegast JM, Rafiei A, et al. Peripheral blood CD34(+) cells efficiently engraft human cytokine knock-in mice. Blood. 2016;128(14):1829-1833.
28. Herold M, Schmalzl F, Zwierzina H. Increased serum interleukin 6 levels in patients with myelodysplastic syndromes. Leuk Res. 1992;16(6-7):585-588.
29. Boada M, Echarte L, Guillermo C, Diaz L, Touriño C, Grille S. 5-Azacytidine restores interleukin 6-increased production in mesenchymal stromal cells from myelodysplastic patients. Hematol Transfus Cell Ther. 2020;43(1):35-42.
30. Yu H, Borsotti C, Schickel JN, et al. A novel humanized mouse model with significant improvement of class-switched, antigen-specific antibody production. Blood. 2017;129(8):959-969.
31. Drexler HG, Dirks WG, Macleod RA. Many are called MDS cell lines: one is chosen. Leuk Res. 2009;33(8):1011-1016.
32. Rhyasen GW, Wunderlich M, Tohyama K, Garcia-Manero G, Mulloy JC, Starczynowski DT. An MDS xenograft model utilizing a patient-derived cell line. Leukemia. 2014;28(5):1142-1145.
33. Tohyama K, Tsutani H, Ueda T, Nakamura T, Yoshida Y. Establishment and characterization of a novel myeloid cell line from the bone marrow of a patient with the myelodysplastic syndrome. Br J Haematol. 1994;87(2):235-242.
34. Muguruma Y, Matsushita H, Yahata T, et al. Establishment of a xenograft model of human myelodysplastic syndromes. Haematologica. 2011;96(4):543-551.
35. Martin MG, Welch JS, Uy GL, et al. Limited engraftment of low-risk myelodysplastic syndrome cells in NOD/SCID gamma-C chain knockout mice. Leukemia. 2010;24(9):1662-1664.
36. Thanopoulou E, Cashman J, Kakagianne T, Eaves A, Zoumbos N, Eaves C. Engraftment of NOD/SCID-beta2 microglobulin null mice with multilineage neoplastic cells from patients with myelodysplastic syndrome. Blood. 2004;103(11):4285-4293.
37. Benito AI, Bryant E, Loken MR, et al. NOD/SCID mice transplanted with marrow from patients with myelodysplastic syndrome (MDS) show long-term propagation of normal but not clonal human precursors. Leuk Res. 2003;27(5):425-436.
38. Wunderlich M, Chou FS, Link KA, et al. AML xenograft efficiency is significantly improved in NOD/SCID-IL2RG mice constitutively expressing human SCF, GM-CSF and IL-3. Leukemia. 2010;24(10):1785-1788.
39. Krevvata M, Shan X, Zhou C, et al. Cytokines increase engraftment of human acute myeloid leukemia cells in immunocompromised mice but not engraftment of human myelodysplastic syndrome cells. Haematologica. 2018;103(6):959-971.
40. Medyouf H, Mossner M, Jann JC, et al. Myelodysplastic cells in patients reprogram mesenchymal stromal cells to establish a transplantable stem cell niche disease unit. Cell Stem Cell. 2014;14(6):824-837.
41. Meunier M, Dussiau C, Mauz N, et al. Molecular dissection of engraftment in a xenograft model of myelodysplastic syndromes. Oncotarget. 2018;9(19):14993-15000.
42. Rouault-Pierre K, Mian SA, Goulard M, et al. Preclinical modeling of myelodysplastic syndromes. Leukemia. 2017;31(12):2702-2708.
43. Moujalled DM, Pomilio G, Ghiurau C, et al. Combining BH3-mimetics to target both BCL-2 and MCL1 has potent activity in pre-clinical models of acute myeloid leukemia. Leukemia. 2018;33(4):905-917.